Visuo-haptic Feedback and Extended Reality in Microinvasive Cardiac Surgery: A Next-Generation Simulator for Mitral Valve Repair

Sofia Breschi[1,†], Domenico Riggio[2,†], Ingrid Tombini[1], Junling Fu[1], Maria Francesca Spadea[2,‡], and Elena De Momi[1,‡]

***Abstract*—Mitral regurgitation is a structural heart disease characterized by dysfunction of the mitral valve. It can be treated through minimally invasive transcatheter edge-to-edge repair procedures, such as those involving the MitraClip™ system. Despite its clinical efficacy, the procedure poses technical challenges, requiring interventional cardiologists to undergo multiple procedures to achieve instrumentation proficiency. Previous studies have demonstrated the efficacy of extended reality simulators in improving surgical skill training. The purpose of this study is to evaluate the effectiveness of visuo-haptic feedback within an extended reality simulator to accelerate and enhance the learning process for the MitraClip™ procedure, potentially offering a valuable tool in surgical training. In this study, based on the prototype of our previous simulator, we further implemented a novel cardiac dynamic environment, a visual feedback interface, an innovative haptic armband, and a new model of the catheter to enhance the simulator's fidelity and educational usability. Experiment results demonstrated that users benefiting from visuo-haptic feedback exhibited significantly reduced completion times, reduced deviation from predefined trajectories, and presented safer navigation results. Moreover, users preferred the visuo-haptic feedback experience, highlighting its perceived value in enhancing training. These findings underscore the potential of adding visuo-haptic feedback to extended reality simulators in surgical training for complex procedures, improving proficiency and patient surgery outcomes.**

***Index Terms*—Medical Robots and Systems, Extended Reality, Surgical Training, Visuo-haptic Feedback, Cardiovascular Surgery.**

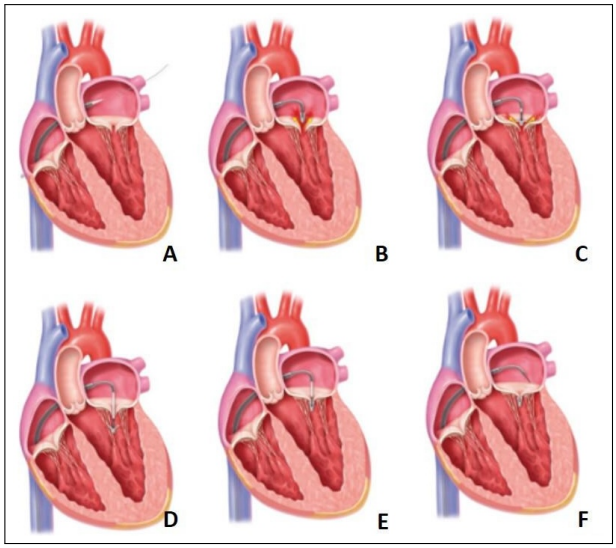

Fig. 1. Phases of the MitraClip™ Procedure. (A) Transseptal puncture: the catheter is introduced into the left atrium through a puncture in the interatrial septum. (B) Advancement of the clip delivery system: the MitraClip™ device is maneuvered into the left atrium and positioned above the mitral valve. (C) Initial alignment: the clip is aligned with the mitral valve leaflets while ensuring proper orientation. (D) Leaflet grasping: the clip arms are opened, and the valve leaflets are captured and secured within the clip. (E) Clip deployment: the MitraClip™ is deployed, creating a double orifice to reduce mitral regurgitation while maintaining proper leaflet coaptation.

I. Introduction

Mitral regurgitation is a structural heart condition resulting from dysfunction of the mitral valve that leads to abnormal backflow of blood from the left ventricle to the left atrium [1]. Opposed to open-heart surgery, this condition can be treated through a group of minimally invasive procedures called Transcatheter Edge-to-Edge Repair (TEER) interventions. An established treatment for this pathology is a percutaneous intervention using the MitraClip™ system (Abbott™ Illinois, U.S.A.), a device designed to apply a clip to the leaflets of the mitral valve through a catheter, thus preventing regurgitant blood flow [2], as depicted in Fig.1. Although effective, this procedure presents significant technical challenges that require a high degree of precision and skill from the interventional cardiologist to maneuver the system and accurate navigation of the device with real-time imaging guidance [3]. Consequently, the success of this intervention is closely linked to the operator's familiarity and dexterity with the MitraClip™ system, skills typically gained through live procedures with real patients [4]. The need to improve procedural training has catalyzed interest in advanced surgical simulators that incorporate extended reality (XR), allowing interventional cardiologists to develop competence in a simulated, risk-free environment. Previous research underscores the potential of XR to enhance surgical training by enabling users to see holograms that mimic the complexities of a real surgical environment [5]. Specifically, we have demonstrated that a Mixed Reality (MR) training simulator facilitated the acquisition of dexterity, enhanced performance, accelerated the learning process, and was more highly appreciated by users in

†These authors contributed equally to this work.
‡These authors contributed equally to this work as senior (co-last) authors.
[1]Department of Electronics, Information and Bioengineering, Politecnico di Milano, Italy. sofia.breschi@polimi.it
[2]Faculty of Electrical Engineering and Information Technology, at the Institute of Biomedical Engineering, Karlsruhe Institute of Technology, Germany. domenico.riggio@kit.edu, publications@ibt.kit.edu
*This work was funded by the European Union - Next Generation EU, and supported by the European Union's Horizon 2020 research and innovation program under the ARTERY project (Grant 101017140).

comparison to real procedure visualization techniques [6]. Yet, while visual immersion alone is beneficial, there is growing evidence that incorporating visuo-haptic feedback into XR simulators can significantly improve the learning experience [7]. In the context of the preceding project [6], the current study aims to enhance the training experience including visual feedback to provide essential spatial orientation cues and haptic feedback to offer information about the potential collision encountered during the procedure. By investigating the impact of these feedback modalities on the users' learning process, we seek to establish a framework for developing XR simulators that replicate the collision and visual intricacies of these procedures. This work ultimately aspires to contribute to the creation of next-generation simulators in mitral valve repair, offering an enriched training tool that can enhance surgical precision and confidence before operating on patients.

II. STATE OF THE ART

A. Simulators and Extended Reality in Surgical Training

Traditional surgical training has historically relied on cadaveric or animal models and expert mentorship to impart essential operative skills. Although effective for hands-on experience, these methods are limited by high costs, ethical considerations, and low repeatability. A seminal meta-analysis underscored the efficacy of technology-enhanced simulation in health professions education, confirming its robust impact on learning outcomes and skill retention [8]. By enabling repeated exposure to realistic yet risk-free scenarios, modern simulators bridge the gap between observational learning in the operating room and the development of operative proficiency, allowing trainees to refine crucial techniques more efficiently. In recent years, advanced surgical simulators and XR technologies have been increasingly adopted [9]. These tools recreate complex surgical environments using patient-specific 3D models and interactive interfaces merged with real surgical tools and design-specific phantoms [10]. Typically, through high-fidelity visuals and dynamic anatomical representations, surgeons can practice and perfect their skills in a controlled setting that mitigates risks. Studies demonstrate that XR platforms accurately replicate procedural steps, deepen anatomical understanding, and enhance psychomotor skills across a range of surgical interventions [11] [9] [12]. Recent systems like the LapAR™ simulator [13], designed for laparoscopic appendectomy training, exemplify this trend by integrating augmented reality overlays with metric-based performance tracking, illustrating the growing adoption of immersive training technologies across surgical disciplines.

B. Training with Extended Reality: Motivations and Limitations

The integration of XR into surgical training provides an innovative platform for bridging the gap between theoretical knowledge and practical skills. XR facilitates real-time overlay of 3D anatomical models on physical environments, enabling surgeons to practice procedures with contextual visualization of patient anatomy. These features have been shown to accelerate learning curves, reduce preparation times, and minimize intraoperative risks [9], [12], [14], [15].

Despite these advantages, XR training faces several challenges. Steep learning curves for adopting the technology and technical limitations such as lag or inaccuracies in real-time model rendering are notable barriers. Additionally, the lack of tactile feedback limits the realism of XR systems, making it difficult to replicate the nuanced physical interactions encountered during surgical procedures. This challenge is also evident in recent AR-based simulators such as LapAR™ [13], which, despite showing efficacy in improving laparoscopic skills, still rely on static anatomical models without dynamic tissue behavior or active haptic integration—limiting their applicability to procedures requiring high-fidelity tactile interaction. So, while XR enhances visual immersion, its potential is limited without the incorporation of advanced haptic feedback mechanisms [16].

C. The Role of Visual and Haptic Feedback

The addition of feedback mechanisms, particularly haptic and visual, has emerged as a critical enhancement for XR simulators. Haptic feedback allows trainees to experience tactile sensations, such as tool resistance, pressure, and anatomical interactions, while visual feedback provides real-time guidance on performance metrics [17]. The combination of these feedback modalities improves user engagement, skill retention, and confidence. Research shows that haptic-enabled simulators improve trainees' understanding of procedural intricacies, reduce errors, and provide a more holistic training experience. For example, in laparoscopic surgery training, force feedback has been shown to improve tool manipulation skills and procedural accuracy [17]–[19]. Particularly, Lin et al. [20] found that virtual reality surgical simulation with haptic integration significantly improved laparoscopic skill acquisition, illustrating how tactile cues can enhance spatial reasoning and manual dexterity. Similarly, temporal bone surgery simulators, that provide real-time feedback, have demonstrated significant improvements in performance and error reduction [21]. These findings underline the critical role of feedback in replicating the tactile and cognitive challenges of real-world surgery, thereby enhancing the educational value of simulators.

D. Applications, Demonstrated Efficacy, and Limitations

XR simulators with visual and haptic feedback have been applied across a range of surgical specialties, including minimally invasive and robotic-assisted procedures. Studies have shown that trainees using feedback-enabled simulators exhibit faster learning curves, reduced errors, and improved procedural outcomes compared to those trained with conventional methods [16], [22]. Despite their promise, these simulators face limitations, such as high computational requirements, restricted availability of high-fidelity haptic devices, and the need for tailored training scenarios to suit specific surgical techniques. For instance, while the LapAR™ [13] simulator demonstrates measurable learning improvements using AR for laparoscopic training, its reliance on static box trainers without

haptic cues or dynamic organ simulation underscores the limitations still present in many current systems. Addressing these constraints will be critical to unlocking the full potential of visuo-haptic feedback in surgical training. In our scenario, complex interventions such as the MitraClip™ procedure, which involves navigating a catheter and manipulating mitral valve leaflets, would benefit greatly from visuo-haptic feedback. Such feedback would aid trainees in mastering intricate maneuvers by warning them of collisions through physical sensations and providing visual guidance associated with the procedure.

In response to the current limitations of XR-based surgical simulators, often focused on isolated aspects such as visual immersion or rigid phantoms, this work presents a comprehensive and highly immersive simulation platform for the MitraClip™ procedure. Our simulator uniquely integrates multiple complementary technologies to enable a training experience that is not only more realistic but also more representative of the cognitive and motor challenges faced during interventional cardiology procedures.

III. Materials and Methods

In our previous work [6], the integration of realistic simulation environments in surgical training has been pivotal in advancing procedural skills, particularly for complex interventions. A state-of-the-art simulator was developed for the MitraClip™ procedure, leveraging both physical and virtual setups to replicate the procedural environment (Fig.2). The developed system combined a cardiovascular anatomical phantom, a support base, and the MitraClip™ delivery system, enhanced by electromagnetic (EM) sensors for tracking and calibration. The phantom was derived from patient-specific CT scans, ensuring anatomical accuracy, while the support base provided stability during simulations.

Specifically, the virtual simulation environment (SE), developed in Unity3D [23], was designed to closely replicate the physical setup, enabling users to interact with a realistic digital twin of the system. The XR interface utilized a head-mounted display (HoloLens 2™ [24]) to provide an immersive 3D representation of the surgical scenario, improving spatial perception and interaction.

Moreover, calibration between the physical and virtual systems was achieved using EM tracking and singular value decomposition techniques to compute T_{EM}^{SE} (Fig.2), ensuring precise correspondence and interaction fidelity. The transformation matrix T_{SE}^{XR} to pair the SE and the XR environment is automatically computed by the XR head-mounted device. The overall communication was managed via the Robotic Operating System (ROS) (Fig.3), optimizing computational efficiency. The calibration scheme is illustrated in Fig. 2. A critical challenge of the approach was the modeling of the catheter's kinematics, allowing realistic simulation of its movement and behavior. The MitraClip™ system exemplifies a Tendon-Driven Continuum Robot, which uses tendons for motion control with three degrees of freedom: translation, anteroposterior bending, and mediolateral bending. Analytical models are essential for designing, analyzing, and controlling such robotic manipulators. Current simulation models for the MitraClip™ catheter include the Variable Curvature model, the Pseudo-Rigid Body model, and the Constant Curvature (CC) model [25]. The latter was chosen for modeling the catheter's kinematics in the simulator. However, while the CC is favoured for real-time applications, it lacks the accuracy required for a realistic representation, especially due to the concentric structure of the catheter and guidewire. In prior simulations, modeling the catheter as a single segment failed to account for the pre-curved nature of the external steerable guide, resulting in simulated curvatures that deviated from reality. To address this, the Piecewise Constant Curvature (PCC) model [26] was introduced. By dividing the catheter into discrete segments, each characterized by constant curvature, the PCC model enables a more accurate simulation of interactions between the catheter and the steerable guide while retaining computational efficiency. Considering the latter as the state of the art simulator, the introduction of comprehensive feedback modalities into such systems could further enhance the training effectiveness, allowing users to access additional information to better understand the tactile and visual nuances of surgical procedures. By building upon this groundwork, future simulators could provide a more immersive and visuo-haptic learning environment, addressing the growing demand for high-fidelity training tools in minimally invasive surgery.

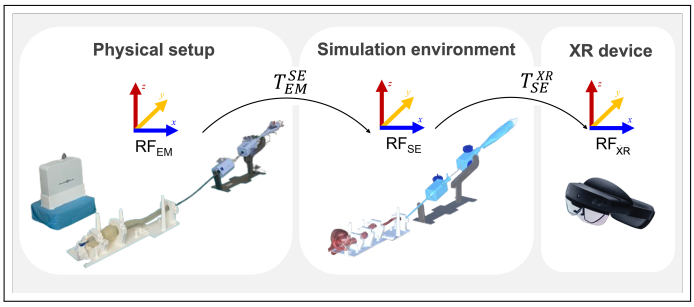

Fig. 2. Illustration of the physical setup, the corresponding digital twin featuring the vein phantom and the respective model, the 3D-printed support base, and the MitraClip™ system.

A. System Overall View

The overall system is presented in Fig.3. The main contributions of this work include (1) a dynamic and realistic heart environment, (2) precise rendering of the catheter, and (3) visuo-haptic feedback that guides and supports catheter navigation during surgical training.

1) Cardiac Setting: A dynamic model of the heart was created using a 4DCT from the 3D Slicer [28] database. A 4DCT is a sequence of many CTs called phases. Specifically, a cardiac 4DCT is a series of CTs gated on the ECG signal. The gating process synchronizes the acquisition of CT images with specific phases of the cardiac cycle.

The process to extract a dynamic model of the heart, that includes all the phases of the 4DCT, began with the segmentation of the anatomical structures in the central phase (5th phase), of the 9-phase included in the 4DCT, using the Total Segmentator module [27] in 3D Slicer [28] (Fig. 4A). Among

all of the extracted structures, only the heart structure and the main vessels were selected (Fig. 4B). Next, the Sequence Registration tool [29] was employed to register the entire 4D image sequence to the chosen reference volume, generating a transform sequence that encodes the evolving 3D displacement field over time (Fig. 4C). This transform sequence was then applied to the reference segmentation, warping the structure contours to the corresponding cardiac phase for all other phases as shown in Fig.4C. The phase-specific segmentations that resulted from the process were then imported into the Blender [30], where they were arranged into a mesh sequence. This sequence was animated generating a cohesive beating-heart motion that reproduces the cardiac cycle. The model was subsequently imported into the simulation environment.

2) Catheter Modeling: In this work, the catheter was modeled using the PCC model, which divides the structure into discrete segments, each defined by its curvature k, angle of the plane containing the arc ϕ, and arc length l (Fig.5).

These parameters are essential for defining the catheter's shape and configuration in anatomical space. The model requires each segment endpoint to be known for performing inverse kinematics. Specifically, the coordinates of the proximal segment's endpoint (x_1, y_1, z_1) are obtained from an electromagnetic (EM) sensor placed on the tip of the external guidewire, while the distal segment's endpoint (x_2, y_2, z_2) is obtained from an EM sensor placed on the catheter's tip. The arc parameters are computed as [31]:

$$\begin{cases} k = \dfrac{2\sqrt{x^2+y^2}}{x^2+y^2+z^2} \\ \phi = \tan^{-1}\left(\dfrac{y}{x}\right) \\ l = \dfrac{\cos^{-1}(1-k\sqrt{x^2+y^2})}{k} \end{cases} \tag{1}$$

Additionally, the segment endpoint coordinates must be expressed relative to their respective segment bases to perform inverse kinematics effectively. Transformation matrices are therefore applied to convert the endpoint coordinates from the global coordinate frame into the local frames of the catheter segments. Specifically, $\mathbf{T}_{i-1}^{i} \in \mathbb{R}^{4\times4}$ is the homogeneous transformation matrix defined as:

$$\mathbf{T}_{i-1}^{i} = \begin{bmatrix} \mathbf{R}_{i-1}^{i} & \mathbf{t}_{i-1}^{i} \\ [0 \quad 0 \quad 0] & 1 \end{bmatrix} \tag{2}$$

where i = 1,2 is the number of segments, $\mathbf{R}_{i-1}^{i} \in \mathbb{R}^{3\times3}$ represents the rotation matrix, and $\mathbf{t}_{i-1}^{i} \in \mathbb{R}^{3}$ denotes the translation vector, respectively.

B. Visuo-haptic Feedback

In the cardiac scenario of the simulator, a critical challenge lies in developing strong spatial awareness, which is essential for acquiring the technical skills required to navigate instruments effectively within the heart's constrained environment [6]. In our proposed framework, visuo-haptic feedback was implemented to enhance the training process. This feedback guides the user through the correct manipulation of the catheter while avoiding proximity to the heart walls. The details of the

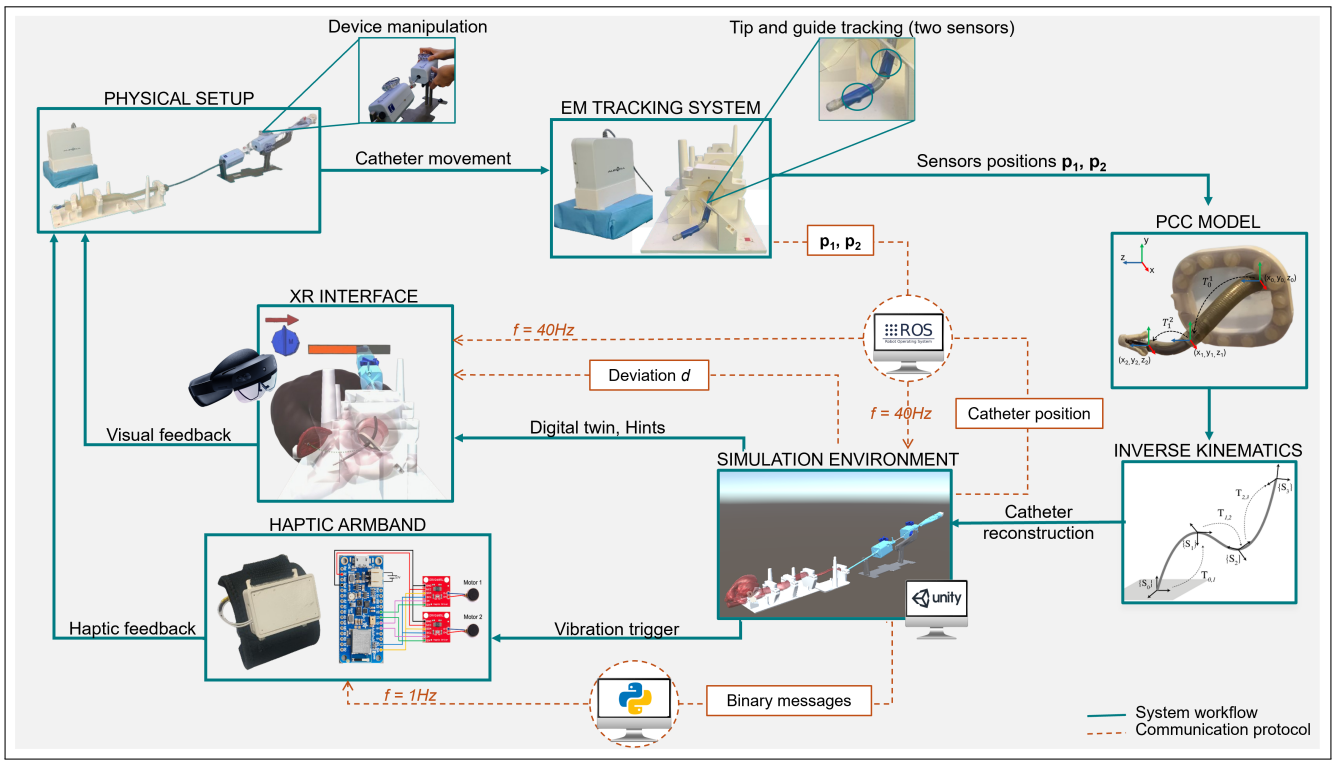

Fig. 3. Block diagram of the overall system and communication protocol.

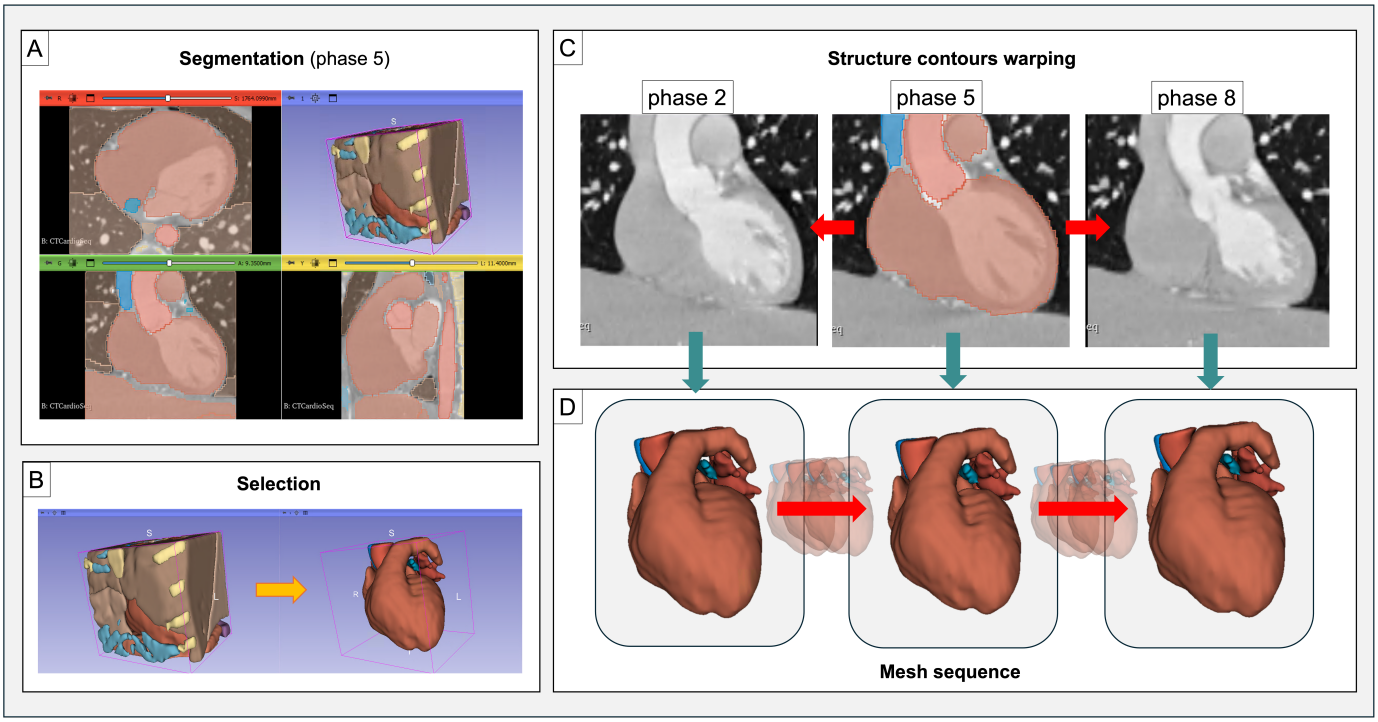

Fig. 4. (A) Total Segmentator [27] in 3D Slicer applied to phase 5, showing automatic segmentation of the structures. (B) Structure selection, isolating the heart and major vessels. (C) Structures contour warping across different cardiac phases (phases 2, 5, and 8), illustrating the propagation of segmented contours to other phases using deformation mapping. (D) Final 3D models of the heart and selected structures for phases 2, 5, and 8.

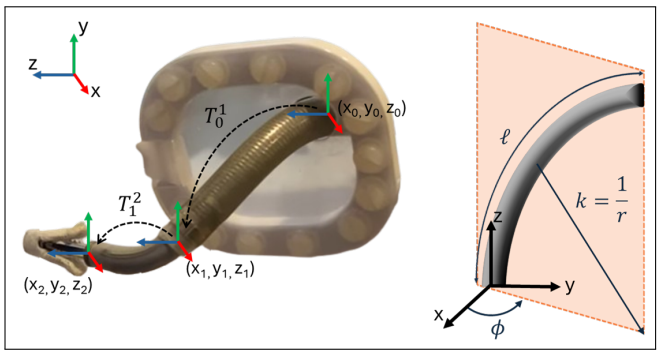

Fig. 5. Left: Model of the catheter as a two-segment PCC. The catheter's base is fixed at the transseptal puncture site (x_0, y_0, z_0). The homogeneous transformation matrices T_{i-1}^{i} are shown. Right: The arc parameters that describe a circular arc, namely curvature k, plane ϕ, and arc length l, are illustrated.

visual and haptic feedback using a self-developed wearable armband are explained below.

1) Visual Feedback: The visual feedback provides real-time hints on how to manipulate the control knobs of the MitraClip™ device, indicating the ideal movements to follow the selected desired trajectory, as presented in Fig. 6. The trajectories, five in total, were derived from the navigation performed by an expert user of the setup, ensuring that they represent optimal paths for the procedure.

Furthermore, in the context of the virtual simulator environment, the deviation d [cm] (Fig. 7), a metric used to quantify the extent to which the catheter's tip movement deviates from a predefined trajectory was computed.

For each position of the catheter's tip, d is calculated as:

$$d = \max\left(0, \min(D_{\max}, d_{\min} - D_{\text{th}})\right) \tag{3}$$

Where:

- $d_{\min}$ represents the minimum distance between the current position of the tip and the trajectory points,
- $D_{\max}$ is the maximum deviation, corresponding to the total distance between the trajectory and the atrial walls in the simulator,
- D_{th} is the maximum allowed distance threshold, approximately one-fourth of $D_{\max}$ in the simulator,
- $\max(0, x)$ ensures that the deviation is not negative,
- $\min(D_{\max}, x)$ limits the deviation to the maximum deviation $D_{\max}$.

The minimum distance $d_{\min}$ [cm] between the current position of the catheter's tip $\mathbf{p}_{\text{tip}}$ and the trajectory points $\mathbf{t}_j$ is defined as:

$$d_{\min} = \min_{j=1}^{M} \|\mathbf{p}_{\text{tip}} - \mathbf{t}_j\| \tag{4}$$

Where:

- $\mathbf{p}_{\text{tip}}$ is the position of the catheter's tip,
- $\mathbf{t}_j$ is the position of the j-th point in the trajectory,
- M is the total number of points that consitute the trajectory,
- $\|\mathbf{p}_{\text{tip}} - \mathbf{t}_j\|$ is the Euclidean distance d between $\mathbf{p}_{\text{tip}}$ and $\mathbf{t}_j$, calculated as:

$$d = \sqrt{(x_{p_{\text{tip}}} - x_{t_j})^2 + (y_{p_{\text{tip}}} - y_{t_j})^2 + (z_{p_{\text{tip}}} - z_{t_j})^2}. \tag{5}$$

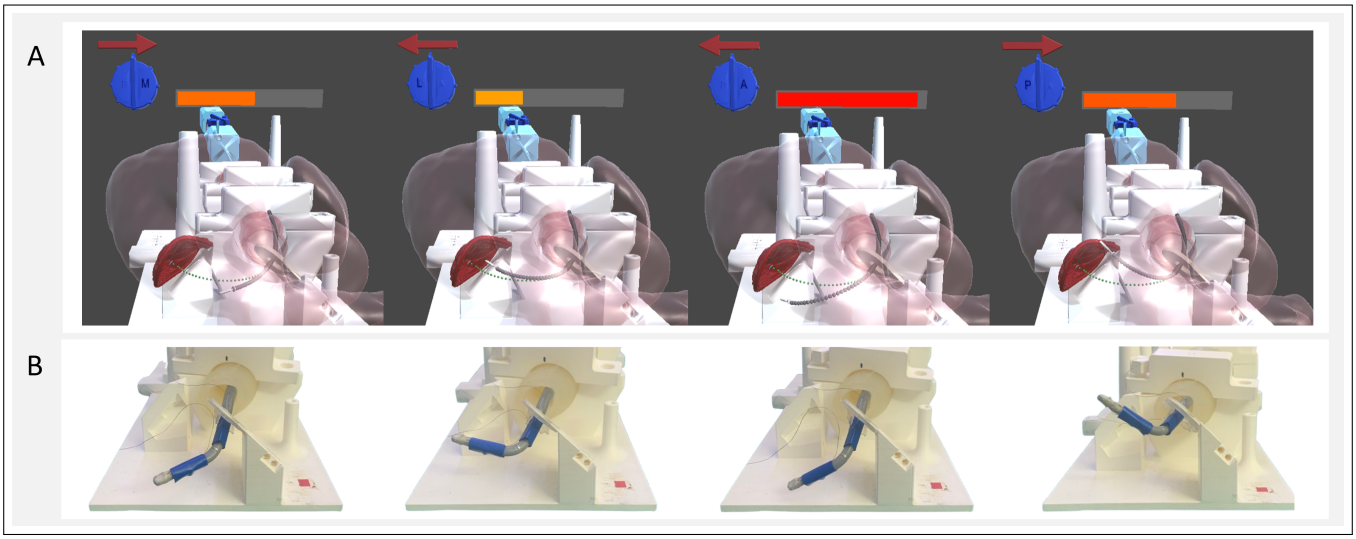

Fig. 6. Representation of the catheter model in the XR virtual environment, along with the visual feedback (A), arranged above its physical counterpart (B). From left to right, the simulator's virtual environment displays the catheter's position within the cardiac setting and its distance from the selected trajectory through a color-coded progress bar. Furthermore, it provides suggestions on which movements to perform to align with the trajectory.

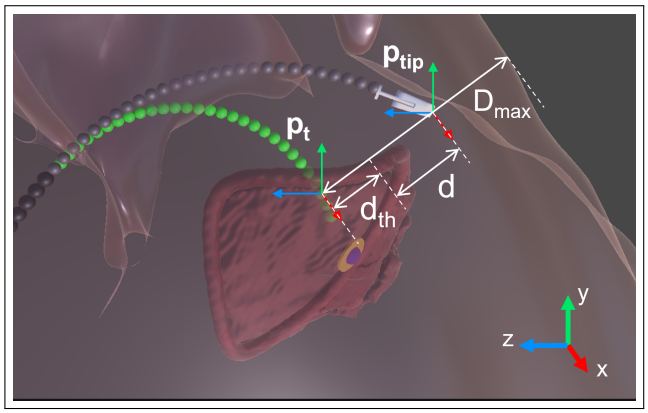

Fig. 7. Illustration reporting the parameters involved in the deviation metric computation. The green-dotted line depicts the trajectory starting from the tip of the steerable guide and ending at a blue-yellow point that represents the target.

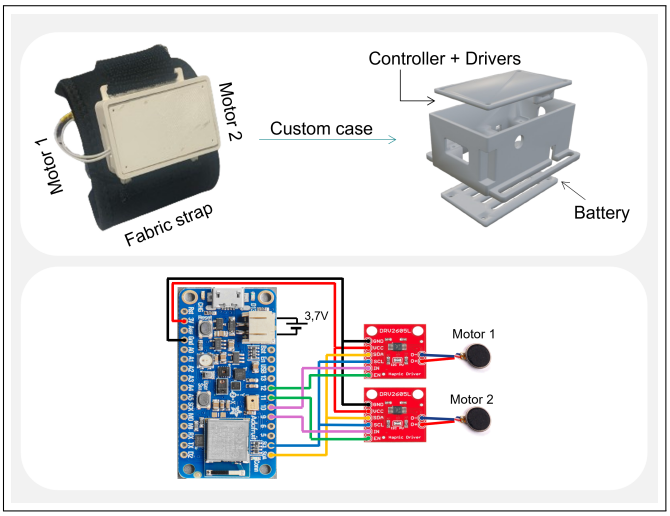

Fig. 8. Custom armband for haptic feedback, equipped with a 3D-printed case containing the microcontroller, two drivers, and the battery, all sewn to a fabric strap along with the two vibration motors.

As illustrated in Fig.6A, a color-coded progress bar displays the deviation extent.

The bar transitions from yellow, indicating minor deviations, to red, signaling significant distance and deviation from the proposed trajectory. Furthermore, an alarm panel gives an alert whenever the catheter comes in contact with the atrial structure. This feature adds other useful information by simulating potential procedural errors and helping users understand the boundaries within the heart. This approach contributes to a more interactive and educational training experience, encouraging the development of precise control and awareness during the training procedure.

2) Haptic Feedback: For more effective learning, the system provides haptic feedback as a warning to signal when near the atrial walls. This feedback is delivered through a proof-of-concept custom armband equipped with vibration motors, as depicted in Fig.8.

Design of the haptic armband: Specifically, the haptic actuation of the armband is realized by two DRV2605L haptic drivers (Texas Instruments, USA), which support both Eccentric Rotating Mass (ERM) and Linear Resonant Actuator (LRA) motors. The DRV2605L features an I²C-controlled playback engine and input with 0% to 100% Duty-Cycle control range. Two miniature ERM motors (FIT0774, 10×2.7mm, 3V DC) are connected to the drivers to deliver localized vibration feedback and ensure sufficient vibration intensity. Furthermore, an Adafruit Feather nRF52840 board (Adafruit Industries, USA) has been employed to deal with the control signal processing and wireless communication, which integrates an ARM® Cortex®-M4F processor (64MHz) and a Bluetooth Low Energy compatible 2.4GHz transceiver.

A lithium-polymer battery (model 502540) rated at 3.7V and 550mAh supplies power to the microcontroller and haptic drivers. The hardware components are housed within a 3D-

printed compact case, which is sewn to a fabric strap along with two vibration motors, as illustrated in Fig.8.

Communication and haptic generation strategy: The communication protocol (please refer to Fig. 3) between the system and the armband is managed through an intermediate Python node, which efficiently handles the computation and delivery of messages. The simulator environment

calculates the proximity of the catheter tip to the heart walls using a collision detection paradigm. Specifically, based on the distance between the catheter tip and the atrial walls, the simulator generates corresponding binary messages and vibration intensities as described in Table.I to inform the human operator of the distance.

TABLE I
TABLE OF THE TRIGGER OF THE MOTOR VIBRATION

Vibration Motors	Distances [cm]		
	$0 \leq d \leq 0.5$	$0.5 < d \leq 1$	$d > 1$
Motor 1	✓	✓	✗
Motor 2	✓	✗	✗

✓, vibration is triggered; ✗, vibration is not triggered;

The vibration signal and messages are transmitted via the workstation's Wi-Fi module and the Python node. Considering the high volume of generated messages, they are aggregated over fixed time intervals of one second, after which only the latest message within each interval will be sent to the armband through the Bluetooth Low Energy (BLE) module. The messages are then interpreted to activate one or both motors, as described in Table.I. The motor control strategy leverages a dual-signal approach through a combination of digital and Pulse Width Modulation (PWM) signals. Digital signals manage the activation state of each motor driver by controlling the *"ENABLE"* pins via digital outputs from the microcontroller. PWM signals are employed to modulate the intensity and speed of each motor by varying the duty cycle of the PWM signal applied to the *"IN"* pins with a frequency of 490 Hz of the motor drivers. For instance, one motor is configured with a duty cycle of approximately 78%, whereas the other one is set to a duty cycle of 100%, ensuring a substantial difference in the perceived vibration intensity between the two motors, enhancing the effectiveness of the haptic feedback.

IV. Experimental Protocol

A. Experimental Setup

1) Task Description: To validate the developed simulator's feasibility and effectiveness, comprehensive user evaluation and comparison experiments have been designed and implemented. Specifically, the participants were asked to navigate the physical catheter using the knobs of the MitraClip™ system, starting from the septum and reaching the target point placed on the mitral valve following the proposed trajectory, and avoiding proximity to the heart walls. As depicted in Fig. 9, the two knobs control the bending of the catheter in the antero-posterior and medio-lateral planes, respectively.

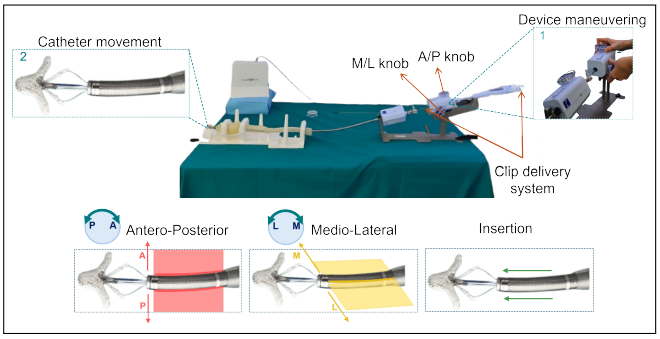

Fig. 9. The MitraClip™ includes a clip delivery system that can be inserted, retracted, and manipulated by the user using the A/P and M/L knobs, which control the bending of the catheter in the corresponding antero/posterior and medio/lateral planes.

Insertion or retraction of the catheter system into the steerable guide is achieved by translating the entire delivery clip system. The head-mounted display used was the Hololens 2™ (Microsoft™, Redmond, U.S.A.) throughout the procedure, providing the visualization of the simulation environment.

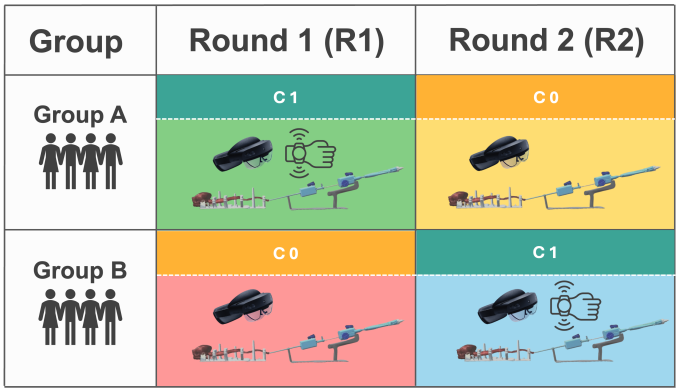

Fig. 10. Users' groups and trials subdivision, where C0 and C1 indicate the five trials conducted without and with visuo-haptic feedback, respectively.

2) Participants: In our experiments, seventeen participants (mean age 26 ± 2.5 years), including a medical resident, were recruited and randomly assigned to two groups: ten participants to Group A and seven participants to Group B.

Specifically, as described in Fig.10, each participant completed two rounds, Round 1 (R1) and Round 2 (R2), with five trials per round, resulting in a total of ten trials per participant. Group A performed R1 with visuo-haptic feedback (Condition "1", C1) and subsequently conducted R2 without it (Condition "0", C0). Conversely, Group B began with R1 and C0, then proceeded to R2 with C1.

Before starting the first trial of R1, each participant received information about the components of the virtual environment and was shown how to manipulate the catheter. After each round, participants were administered a questionnaire to evaluate their subjective perception of the simulation environment under conditions C1 and C0. At the end of both rounds R1 and R2, the users were asked to express a preference between the experience with visuo-haptic feedback and without it. All participants provided informed consent prior to participation,

and the experimental protocol was approved by the Ethics Committee of Politecnico di Milano, Italy (No. 45/2023).

B. Performance Metrics

To investigate the usability evaluation of the developed simulator for mitral valve repair training, the following metrics have been recorded and primarily consist of:

(1) Completion time T_c [s] was computed as the difference between the start of the trial T_0 and the end of the trial T_f.

$$T_c = T_f - T_0 \tag{6}$$

(2) Deviation percentage *dev* [%], which is a normalized metric that evaluates how far the catheter's tip strays from a predefined trajectory over time. This percentage provides a representation of the average deviation relative to the maximum deviation $D_{\max}$ (please refer to Subsection III-B), across multiple recorded samples N:

$$dev = \left(\frac{\sum_{i=1}^{N} d_i}{N \cdot D_{\max}} \right) \cdot 100\% \tag{7}$$

Where:

- $\sum_{i=1}^{N} d_i$ is the sum of accumulated deviations d (Eq. 3) across multiple samples over time,
- N is the number of recorded deviation samples,
- $D_{\max}$ is the maximum deviation, corresponding to the total distance between the proposed trajectory and the atrial walls in the simulator.

(3) Risk factor R_f is defined as the sum of the binary messages generated by the simulator that trigger the vibration for the haptic feedback (please refer to Subsection III-B):

$$R_{\mathrm{f}} = \sum \#m \tag{8}$$

where:

- $\#m$ is the number of binary messages generated by the simulator over time that trigger the vibration of at least one motor.

(4) The NASA Task Load Index (NASA-TLX) questionnaire was employed to assess the user-perceived workload during the experiments using different control modalities for task completion [32].

C. Data Processing and Analysis

After data collection, analyses were conducted to determine whether the metrics provided evidence for differences between the experiences with C0 and C1, influenced by the impact of visuo-haptic feedback. All statistical analyses described in the following sections used a conventional significance threshold of $\alpha = 0.05$ for each test performed.

As a first step, the analyses aimed to assess whether participants in Group A showed performance improvements from R1 to R2. This was evaluated both across the five trials individually and by considering the overall data for rounds 1 and 2. Data distribution was visualized using box plots for Group A and Group B. Additionally, two learning curves depicting median values and percentiles (one for R1 and one for R2) were generated for each group across trials 1 to 5. Finally, a nonparametric Mann–Whitney U test was performed to determine whether pairwise comparisons between corresponding trials of R1 and R2 (e.g., Trial 1 in R1 vs. Trial 1 in R2, etc.) and between the overall rounds (R1 vs. R2) for each group (A and B) showed statistically significant differences.

If no statistically significant differences were observed between R1 and R2, the two groups were analyzed separately and divided into two new datasets based on condition types C0 and C1. Box plots were then created for each dataset to illustrate the distributions, and the differences were tested for statistical significance as described earlier.

Finally, in the case of non-significant results, a Kruskal–Wallis test was applied to assess whether the data, when considering C1 and C0, exhibited different trends across the learning curves.

V. Experiment Results and Discussion

Comprehensive processing and statistical analyses were performed on the data collected during the experimental phase, as described in Subsection IV-C. Fig. 11 summarizes all the results obtained for task completion time, trajectory deviation, and risk factor.

1) Comparison of Task Completion Time Results: Following statistical analyses, the data revealed that in Group A, the first three trial comparisons between R1 and R2 indicated a statistically significant improvement in completion time during R2, as evidenced by lower median values (Fig. 11A and Fig. 11B). These findings suggest that the use of visuo-haptic feedback in R1 may have facilitated a carryover effect, improving dexterity and efficiency when the participants performed the second round without visuo-haptic feedback. The last two box plots of the curve in Fig. 11A didn't show any significant change, and the trend of the curves in Fig. 11B shows that the completion time looks to reach a plateau in the last two trials possibly due to the minimum needed time to complete the task. This may be attributed to a limitation of the system, which provided overall simple navigation paths without obstacles and did not require particularly complex movements. A similar procedure was conducted for Group B to evaluate whether performance improvements occurred from R1 to R2. As before, box plots and learning curves in Fig. 11E and 11F of completion time are reported. The comparisons revealed no statistically significant differences in any of the trials. These findings may suggest that, for Group B, the first round with C0 did not confer a measurable carryover benefit in subsequent performance during the second round with C1. Supporting these results, Fig. 11C confirms the observed learning trend also when considering the overall data of R1 and R2 for Group A, while Fig. 11G shows no differences between rounds for Group B.

2) Deviation Percentage Results: The statistical analysis indicated no significant differences between R1 and R2 for both groups A and B. The main cause for this outcome may be the limited number of participants in the experiments, as well as the restricted available space in the cardiac environment of the simulator between the proposed trajectories

and the atrial walls, leading to very similar deviation values. Consequently, the two groups were analyzed separately and organized into two new datasets based on condition type. The results illustrated in Fig. 11D show notable differences between the experiments conducted with C0 and C1, with the median deviation being lower for C1. These findings suggest that visuo-haptic feedback, particularly the visual component, improved navigation precision, as reflected by the reduced deviation values.

3) Risk factor: To investigate the effects of the visuo-haptic feedback on perceived procedural risk, the metric risk factor was analyzed following the same structured statistical procedure. First, separate comparisons were conducted between R1 and R2 of every group. These initial analyses revealed no statistically significant differences between the rounds within the respective groups. The data were then split into two different datasets based on condition type. For each of these datasets, a learning curve was generated (Fig. 11F). Subsequent tests revealed that there were no significant differences between the corresponding trials across the two datasets.

These results should be attributed, as before, to the limited participant pool, the narrow space available within the cardiac environment, and the wear of the MitraClip™ system, which impairs its functionality. Moreover, a short distance between the chosen trajectory and the heart walls facilitates the activation of haptic feedback unless the users have sufficiently learned to follow the trajectory accurately. Despite the absence of per-trial differences, a further analysis was carried out to assess whether the risk factor data exhibited different trends across the learning curves. For the dataset with C1, significant differences along the trial sequence were detected, indicating a decreasing trend over time. This pattern suggests that the visuo-haptic feedback, particularly the haptic component, facilitated a learning process in risk management. In contrast, the dataset with C0 did not show any significant trend across trials, implying that participants did not progressively modify their risk levels in the absence of feedback. Overall, these findings indicate that while individual trial comparisons between C0 and C1 did not differ significantly, the dynamic analysis of the learning curve points to an improvement in navigational safety attributable to visuo-haptic feedback.

4) Qualitative Evaluation Results: To evaluate the impact of visuo-haptic feedback on participants' subjective experience during catheter navigation, the NASA-TLX scores were analyzed. Average scores across the metrics, such as Mental Demand, Physical Demand, Temporal Demand, Performance, Effort, and Frustration, showed no significant differences between C0 and C1 conditions, as displayed in Fig.12 and 13. This suggests that participants perceived both systems equally and positively, confirming the use and effectiveness of XR in surgical training.

These results reflect the participants' ability to adapt quickly to the system throughout the trials and that the simulation environment was effectively implemented, thereby strengthening the findings of previous work [6].

As participants became more familiar with the task and interface, their perceived improvement due to practice may have overshadowed actual advantages provided by feedback demonstrated by the quantitative analysis of the results. However, most participants (15 out of 17) rated the overall training experience with visuo-haptic feedback more favorably than without it, while only one participant preferred the setup without visuo-haptic feedback, and another remained indifferent.

Overall, the positive scores across all dimensions point to a general acceptance of the XR simulation environment, highlighting its usability and effectiveness in providing a satisfactory training experience.

VI. CONCLUSIONS

Firstly, a key aspect of a simulator is its level of realism and fidelity to mimic the physical scenarios for Mitral Valve Re-

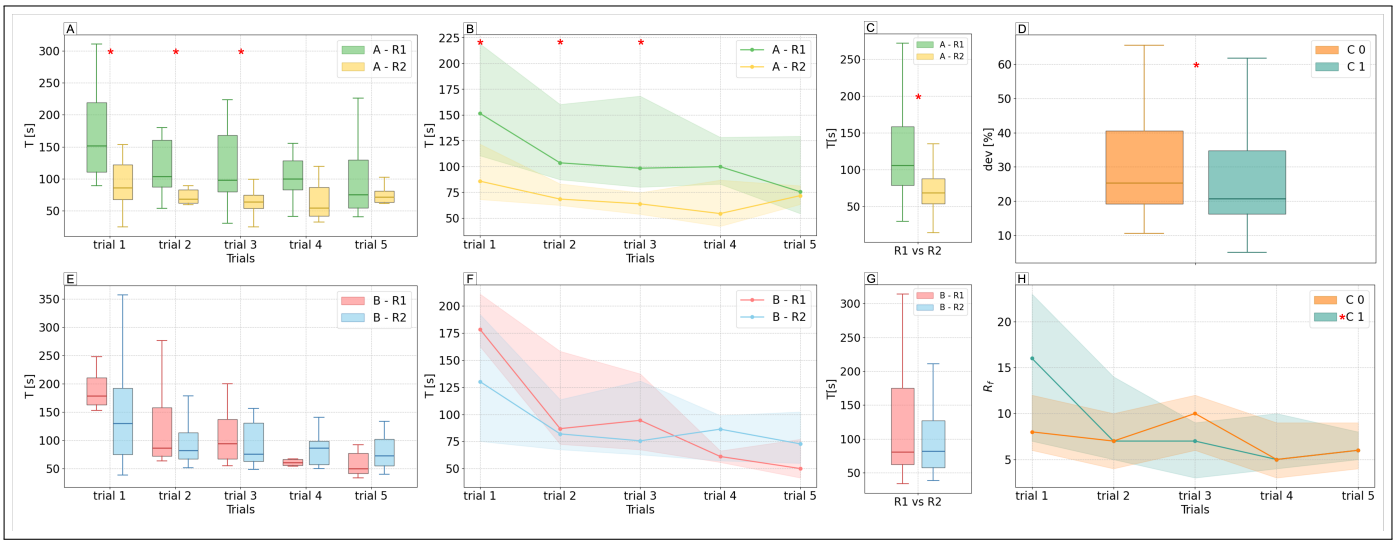

Fig. 11. A) Group A, R1 vs R2 trials distribution boxplots. B) Group A, R1 vs R2 learning curve with interquartile range. C) Group A, R1 vs R2 distribution boxplots. D) Deviation distribution boxplots of C0 and C1. E) Group B, R1 vs R2 trials distribution boxplots. F) Group B, R1 vs R2 learning curve with interquartile range. G) Group B, R1 vs R2 distribution boxplots. H) Risk factor learning curves of C0 and C1 divided per trials.

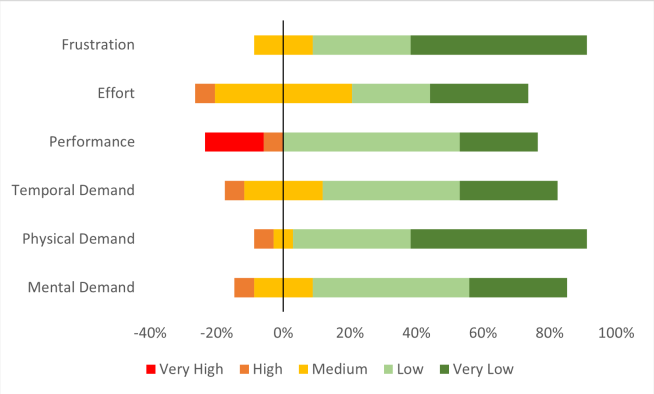

Fig. 12. Representation of NASA-TLX questionnaire results using a Likert scale for experiments conducted without feedback (C0), where lower scores represent better evaluations.

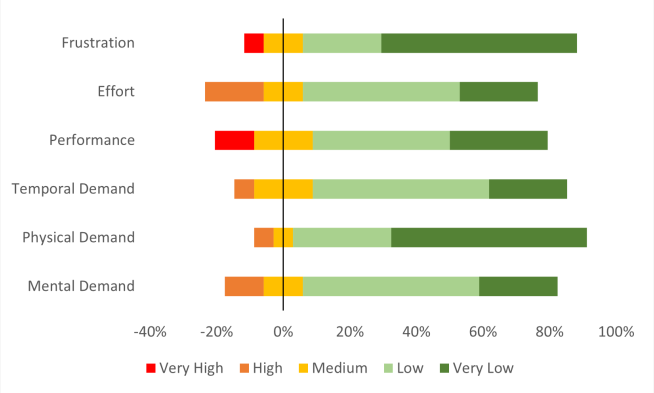

Fig. 13. Likert chart of NASA-TLX questionnaire results for evaluating visuo-haptic feedback (C1), where lower scores indicate better evaluations on the utilized scale

pair surgical procedures. Specifically, the proposed simulator integrates the dynamic 3D heart environment, and advanced catheter modeling enhances the simulation's adherence to reality, thereby providing a valid tool for surgical training. Specifically, the cardiac dynamic model incorporates a lifelike beating heart motion that mimics the cardiac cycle, allowing users to experience the challenges of the procedure from the early stages of training. Additionally, the representation of the virtual catheter using a PCC model allows for a good trade-off between accuracy and real-time kinematics computation requirements. The PCC model divides the device into two distinct segments, enabling precise tracking and reconstruction within the simulator. Compared to a single curvature segment, the dual-curvature approach offers a more accurate portrayal of the catheter by replicating the pre-curved shape of the external steerable guide, thereby capturing the interaction between the two segments, which rely on each other as the catheter is placed within the guide wire. Moreover, the effectiveness of integrating visuo-haptic feedback into an XR simulator for training interventional cardiologists in the MitraClip™ procedure has been investigated. The primary objective was to explore whether the inclusion of both visual and haptic modalities could enhance the learning process, improve procedural accuracy, and increase user confidence compared to the visual feedback alone.

Despite significant advances in XR visualization and standalone haptic trainers, existing platforms generally address only one dimension of immersive surgical simulation, dynamic anatomy, real-time force feedback, or visual guidance, without unifying them in a single, user-driven system or placing them in the clinical context of TEER procedures. Our work fills this gap by combining a dynamic XR cardiac environment, accurate continuum-robot catheter modeling, real-time visual cues, and wearable vibrotactile feedback into one cohesive simulator. This integrated approach delivers measurable improvements in procedural speed, precision, and safety, marking an evolution beyond what current simulators offer.

In the broader context of AR-based surgical simulation, our findings align with an interesting new study, the LapAR™ simulator [13], developed for laparoscopic appendectomy training, which leverages augmented reality overlays and collects quantitative performance metrics such as procedure time, instrument path length, and motion smoothness to assess skill acquisition over repeated trials. Although the clinical focus differs laparoscopy versus transcatheter intracardiac procedures, the validation methodology and metric-driven evaluation approach are conceptually aligned with our work. Both systems emphasize reproducibility, immersive environments, and data-driven feedback to support technical skill development. However, due to the substantial differences in anatomical context, procedural objectives, and tool dynamics, direct comparisons of performance outcomes are not applicable. Nonetheless, the LapAR™ study reinforces the relevance and timeliness of immersive, AR-enhanced platforms in surgical education, supporting the direction and novelty of our proposed simulator.

The experimental results demonstrated that participants who engaged with the simulator incorporating visuo-haptic feedback (Group A) exhibited significant improvements in completion time from R1 to R2, suggesting that the initial exposure to comprehensive feedback facilitated a faster learning curve. Additionally, the deviation metric revealed that trials conducted with visuo-haptic feedback consistently resulted in lower deviations from the optimal trajectory, indicating enhanced navigation precision. Finally, the analysis of the learning curves for the risk factor points to an enhancement in navigational safety, thanks to visuo-haptic feedback.

These outcomes highlight the potential advantage of introducing visuo-haptic feedback early in the training process to maximize its benefits. Despite the observed quantitative advantages, the NASA-TLX assessments indicated no significant differences in perceived workload between the feedback and non-feedback conditions, however, confirming the effectiveness of a simulation environment that leverages XR. Furthermore, qualitative feedback revealed a general preference for the visuo-haptic system, underscoring its perceived value in enhancing the overall training experience. These findings highlight the importance of integrating multi-modal feedback mechanisms into surgical simulators to foster more effective and efficient skill acquisition, potentially translating to better clinical outcomes and increased patient safety in real-world applications.

Nevertheless, it is important to acknowledge several limitations in this work, which considered a restricted pool of

users and did not include expert interventional cardiologists in the experiments. Furthermore, as previously discussed, the wear of the MitraClip™ system and the confined space within the simulator's cardiac environment may have influenced the experimental outcomes, leaving room for improvements.

Future developments will focus on further increasing the simulator's realism and clinical relevance. A key direction will be the integration of deformable models, although not critical for this initial validation phase, such models would allow simulation of various and realistic scenarios, particularly in cases involving close contact between the catheter and dynamic cardiac structures. This enhancement would be especially valuable when simulating the full procedural pathway, including venous access, transseptal puncture, and vascular navigation.

A second line of future work involves the evaluation of the simulator with interventional cardiologists, who are the actual end-users of the MitraClip™ procedure. While this study used non-medical expert participants to assess usability and technical effectiveness, upcoming clinical studies will investigate the training impact of the simulator in medical settings.

Ultimately, future developments should explore the scalability of the system across various surgical procedures, and adaptive feedback mechanisms tailored to individual learning paces to further optimize the training process.

ACKNOWLEDGMENTS

The authors would like to express their gratitude to all the participants in the experiment.

REFERENCES

[1] I. Karagodin, A. Singh, and R. M. Lang, "Pathoanatomy of mitral regurgitation," *Structural Heart*, vol. 4, no. 4, pp. 254–263, 2020.

[2] A. Perlowski and T. Feldman, "Percutaneous treatment of mitral regurgitation: The mitraclip experience," *Interventional Cardiology Clinics*, jan 2012.

[3] M. A. Sherif, L. Paranskaya, S. Yuecel, S. Kische, O. Thiele, G. D'Ancona, A. Neuhausen-Abramkina, J. Ortak, H. Ince, and A. Öner, "Mitraclip step by step; how to simplify the procedure," *Netherlands Heart Journal*, 2017.

[4] A. K. Chhatriwalla, S. Vemulapalli, D. R. J. Holmes, D. Dai, Z. Li, G. Ailawadi, D. Glower, S. Kar, M. J. Mack, J. Rymer, A. S. Kosinski, and P. Sorajja, "Institutional experience with transcatheter mitral valve repair and clinical outcomes: Insights from the tvt registry," *JACC Cardiovascular Interventions*, vol. 12, no. 14, pp. 1342–1352, 2019.

[5] A. J. Lungu, W. Swinkels, L. Claesen, P. Tu, J. Egger, and X. Chen, "A review on the applications of virtual reality, augmented reality and mixed reality in surgical simulation: an extension to different kinds of surgery," *Expert Review of Medical Devices*, vol. 18, no. 1, pp. 47–62, 2021.

[6] D. Riggio, S. Breschi, A. Peloso, M. F. Spadea, and E. De Momi, "Augmented reality in microinvasive cardiac surgery: Towards a training simulator for mitral valve repair intervention," in *2024 10th IEEE RAS/EMBS International Conference for Biomedical Robotics and Biomechatronics (BioRob)*, 2024, pp. 1727–1732.

[7] F. G. Hamza-Lup, C. M. Bogdan, D. M. Popovici, and O. D. Costea, "A survey of visuo-haptic simulation in surgical training," *International Conference on Mobile, Hybrid, and Online Learning*, 2019. [Online]. Available: https://arxiv.org/abs/1903.03272

[8] D. A. Cook, R. Hatala, R. Brydges, B. Zendejas, S. J. Hamstra, and V. D. Bryson, "Technology-enhanced simulation for health professions education: A systematic review and meta-analysis," *JAMA*, vol. 306, no. 9, pp. 978–988, 2011.

[9] J. W. Yoon, R. E. Chen, E. J. Kim, O. O. Akinduro, P. Kerezoudis, P. K. Han, and et al., "Augmented reality for the surgeon: systematic review," *International Journal of Medical Robotics*, vol. 14, p. e1914, 2018.

[10] J. Fu, M. Pecorella, E. Iovene, M. C. Palumbo, A. Rota, A. Redaelli, G. Ferrigno, and E. De Momi, "Augmented reality and human–robot collaboration framework for percutaneous nephrolithotomy: System design, implementation, and performance metrics," *IEEE Robotics & Automation Magazine*, 2024.

[11] D. Cannizzaro, S. K. Rammos, S. Peschillo, A. M. El-Nashar, A. W. Grande, and G. Lanzino, "The lateral mesencephalic vein: surgical anatomy and its role in the drainage of tentorial dural arteriovenous fistulae," *World Neurosurgery*, vol. 85, pp. 163–168, 2016.

[12] D. Cannizzaro, I. Zaed, A. Safa, A. J. M. Jelmoni, A. Composto, A. Bisoglio, and et al., "Augmented reality in neurosurgery, state of art and future projections. a systematic review," *Frontiers in Surgery*, 2022.

[13] S. Colman, M. El-Bahnasawi, N. Abdulkader, Z. Aloul, J. Brown, P. Luthra, and D. Rawaf, "The 'lapar' augmented reality training device in surgical simulation: a multi-center pilot study," *Global Surgical Education - Journal of the Association for Surgical Education*, vol. 4, no. 32, pp. 1–20, 2025. [Online]. Available: https://doi.org/10.1007/s44186-024-00343-5

[14] B. In, "Augmented and virtual reality in surgery," https://builtin.com/healthcare-technology/augmented-virtual-reality-surgery, 2024, accessed: 2024-12-27.

[15] F. Cofano, G. Di Perna, M. Bozzaro, A. Longo, N. Marengo, F. Zenga, and et al., "Augmented reality in medical practice: from spine surgery to remote assistance," *Frontiers in Surgery*, vol. 8, p. 657901, 2021.

[16] R. R. McKnight, C. A. Pean, J. S. Buck, J. S. Hwang, J. R. Hsu, and S. N. Pierrie, "Virtual reality and augmented reality-translating surgical training into surgical technique," *Current Reviews in Musculoskeletal Medicine*, vol. 13, pp. 663–674, 2020.

[17] E. M. Overtoom, T. Horeman, F. W. Jansen, J. Dankelman, and H. W. R. Schreuder, "Haptic feedback, force feedback, and force-sensing in simulation training for laparoscopy: A systematic overview," *Journal of Surgical Education*, vol. 76, no. 1, pp. 242–261, 2018.

[18] M. Zhou, S. Tse, A. Derevianko, D. B. Jones, S. D. Schwaitzberg, and C. G. L. Cao, "Effect of haptic feedback in laparoscopic surgery skill acquisition," *Surgical Endoscopy*, vol. 26, no. 4, pp. 1128–1134, 2012.

[19] K. Rangarajan, H. Davis, and P. H. Pucher, "Systematic review of virtual haptics in surgical simulation: A valid educational tool?" *Journal of Surgical Education*, vol. 77, no. 2, pp. 337–347, 2019.

[20] X. Lin, M. Chen, Y. Zhang, D. Gong, and J. Cai, "Virtual reality surgical simulation for training of laparoscopic surgery: A systematic review," *Journal of Computer Assisted Tomography*, vol. 43, no. 5, pp. 776–780, 2019.

[21] S. Wijewickrema, I. Ioannou, Y. Zhou, P. Piromchai, J. Bailey, G. Kennedy, and S. O'Leary, "A temporal bone surgery simulator with real-time feedback for surgical training," in *Medicine Meets Virtual Reality 21*, ser. Studies in Health Technology and Informatics. IOS Press, 2013, vol. 196, pp. 462–468.

[22] E. Boyle, M. Al-Akash, A. G. Gallagher, O. Traynor, A. D. K. Hill, and P. C. Neary, "Optimising surgical training: use of feedback to reduce errors during a simulated surgical procedure," *Postgraduate Medical Journal*, vol. 87, no. 1030, pp. 524–528, 06 2011. [Online]. Available: https://doi.org/10.1136/pgmj.2010.109363

[23] U. Technologies, "Unity engine," https://unity.com, 2024, accessed: 2024-12-27.

[24] Microsoft, "Hololens 2," https://www.microsoft.com/en-gb/d/hololens-2/91pnzzznzwcp?msockid=20cbc708c7916bf70eb7d3c9c6e66a9b&activetab=pivot:overviewtab, 2024, accessed: 2024-12-27.

[25] P. Rao, Q. Peyron, S. Lilge, and J. Burgner-Kahrs, "How to model tendon-driven continuum robots and benchmark modelling performance," *Frontiers in Robotics and AI*, vol. 7, p. 630245, 2021.

[26] B. Jones and I. Walker, "Kinematics for multisection continuum robots," *IEEE Transactions on Robotics*, vol. 22, no. 1, pp. 43–55, 2006.

[27] J. Wasserthal, H.-C. Breit, M. T. Meyer, M. Pradella, D. Hinck, A. W. Sauter, T. Heye, D. T. Boll, J. Cyriac, S. Yang, M. Bach, and M. Segeroth, "Totalsegmentator: Robust segmentation of 104 anatomic structures in ct images," *Radiology: Artificial Intelligence*, vol. 5, no. 5, Sep. 2023. [Online]. Available: http://dx.doi.org/10.1148/ryai.230024

[28] "3d slicer," https://www.slicer.org.

[29] YouTube, "Mr procedure," https://https://github.com/moselhy/SlicerSequenceRegistration, 2024, accessed: 2024-12-27.

[30] "Blender," ://www.blender.org/.

[31] G. Zhong, B. Peng, and W. Dou, "Kinematics analysis and trajectory planning of a continuum manipulator," *International Journal of Mechanical Sciences*, vol. 223, p. 107206, 2022.

[32] S. G. Hart, "Nasa-task load index (nasa-tlx); 20 years later," in *Proceedings of the human factors and ergonomics society annual meeting*, vol. 50, no. 9. Sage publications Sage CA: Los Angeles, CA, 2006, pp. 904–908.